

Chaos in the Takens–Bogdanov bifurcation with $O(2)$ symmetry

A. M. Rucklidge, Department of Applied Mathematics, University of Leeds,
Leeds LS2 9JT, UK

E. Knobloch, Department of Physics, University of California,
Berkeley CA 94720, USA

(February 7, 2022– DOI:)

The Takens–Bogdanov bifurcation is a codimension two bifurcation that provides a key to the presence of complex dynamics in many systems of physical interest. When the system is translation-invariant in one spatial dimension with no left-right preference the imposition of periodic boundary conditions leads to the Takens–Bogdanov bifurcation with $O(2)$ symmetry. This bifurcation, analyzed by G. Dangelmayr and E. Knobloch, *Phil. Trans. R. Soc. London A* **322**, 243 (1987), describes the interaction between steady states and traveling and standing waves in the nonlinear regime and predicts the presence of modulated traveling waves as well. The analysis reveals the presence of several global bifurcations near which the averaging method (used in the original analysis) fails. We show here, using a combination of numerical continuation and the construction of appropriate return maps, that near the global bifurcation that terminates the branch of modulated traveling waves, the normal form for the Takens–Bogdanov bifurcation admits cascades of period-doubling bifurcations as well as chaotic dynamics of Shil’nikov type. Thus chaos is present arbitrarily close to the codimension two point.

1 Introduction

When a layer of fluid is heated from below, steady convection sets in once the temperature difference across the layer exceeds a critical value, destabilizing the fluid by buoyancy effects. If sufficiently strong competing stabilizing effects are included the initial instability can be oscillatory [1], and the associated dynamics become much more interesting. This behavior is organized by the Takens–Bogdanov (TB) bifurcation that occurs when the primary bifurcation

changes from a pitchfork bifurcation (leading to steady convection) to a Hopf bifurcation (leading to oscillatory convection with the same wavenumber). This codimension-two bifurcation arises in a wide variety of convection problems, including thermosolutal convection, magnetoconvection, binary fluid convection and rotating convection [2–7], as well as other problems of physical interest such as Langmuir circulation [8], coupled oscillators [9], and the formation of spiral waves in chemical reactions [10].

The linearized dynamics at the Takens–Bogdanov bifurcation are characterized by the matrix $\begin{bmatrix} 0 & 1 \\ 0 & 0 \end{bmatrix}$, but the exact form of the normal form equations that describe the nonlinear dynamics near the codimension-two bifurcation point depends critically on the symmetry of the problem. Even without any symmetry, the existence of a global (homoclinic) bifurcation may be deduced, and the case of simple reflection (Z_2) symmetry is also well understood [2, 11]. Neither of these cases exhibits chaos since the normal forms are two-dimensional. However, even relatively simple extensions (for example, to D_3 and D_4 symmetry [12, 13]) do exhibit chaotic dynamics within the corresponding normal form although the details remain to be fully understood.

We are interested here in the case of circular $O(2)$ symmetry, which is relevant to two-dimensional convection with periodic boundary conditions in the horizontal. The analysis of Dangelmayr and Knobloch [14] (hereafter DK) of the fourth-order normal form for this problem revealed a wide variety of competing states, including standing waves (SW), traveling waves (TW), modulated waves (MW) and steady-state convection (SS), and catalogued possible transitions between these states and the trivial (zero) solution. However, DK found no chaotic dynamics near the codimension-two point, which is at first glance surprising given that the ordinary differential equations (ODEs) describing the dynamics are of fourth order. However, one phase variable decouples (reducing the order to three), and DK used an averaging procedure to reduce the order from three to two, which excludes the possibility of chaotic dynamics. This procedure gives the correct description of the dynamics close to the codimension-two bifurcation point, but it makes assumptions about the time scales in the problem that are not valid near global bifurcations. This does not cause problems in the case of global bifurcations of SW, where the dynamics remain confined to a two-dimensional reflection-invariant subspace, but one of the situations they discussed, in which a MW is created in a Hopf

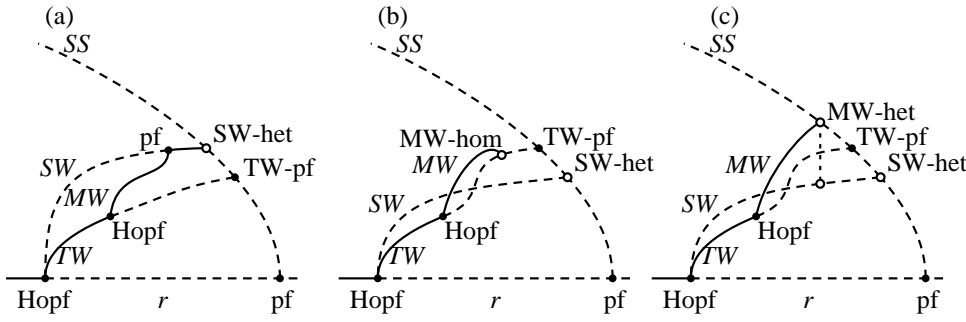


Figure 1. Three scenarios for the ending of the MW branch: (a) in a pitchfork bifurcation with the SW branch; (b) in a global bifurcation with the TW branch; (c) in a global bifurcation with the SW and SS branches. Diagrams (a) and (b) are characteristic of parameter regions labeled III^- and II^- by DK [14, figure 5], although (b) turns out not to be correct; (c) is as in [15].

bifurcation from a TW, and is then destroyed when it collides with the same TW in a global bifurcation, is topologically impossible in second-order problems.

In this paper, we examine in some detail the ways in which the branch of MW can terminate. The two possibilities described by DK are that it ends in a pitchfork bifurcation on the SW branch (Figure 1a) or in a global bifurcation when it collides with TW (Figure 1b). We show that this global bifurcation is associated with chaotic dynamics in the normal form (and hence in physical problems described by the normal form) arbitrarily close to the codimension-two point. We also find that farther from the codimension-two point, the branch of MW can end in a global bifurcation involving the SS and SW solutions (Figure 1c); this scenario has been found in [8, 15, 16], but it was not previously known to occur in the normal form. However, this global bifurcation cannot be brought arbitrarily close to the codimension-two point, and so is not strictly within the realm of validity of the normal form.

This paper is organized as follows. In section 2 we summarize the normal form equations and their basic properties; in section 3 we describe our results obtained by a combination of numerical continuation using AUTO and direct integration of the ODEs, and in section 4 we construct a two-dimensional map in order to analyse the dynamics near the coincidence of the pitchfork bifurcation from SS to TW and the heteroclinic bifurcation in which the SW collide with the SS equilibria. In section 5 we discuss the significance of our findings.

2 Equations

In the motivating physical problems, the state that bifurcates from the trivial solution is characterized by a complex amplitude $v(t)$ multiplying the marginal eigenfunction with horizontal wavenumber k . In a periodic domain of width $\lambda = 2\pi/k$ invariance of the problem under translations ($x \rightarrow x + d$) and left–right reflection ($x \rightarrow \lambda - x$) induces the following action of $O(2)$ on the amplitude v :

$$v \rightarrow e^{ikd}v, \quad v \rightarrow \bar{v}. \quad (1)$$

The normal form of the Takens–Bogdanov bifurcation with $O(2)$ symmetry, truncated at cubic order, is:

$$\ddot{v} = \mu v + \nu \dot{v} + A|v|^2v + B|\dot{v}|^2v + C(v\dot{v} + \bar{v}\dot{v})v + D|v|^2\dot{v}, \quad (2)$$

where μ and ν are unfolding parameters, and A , B , C and D are real constants [14]. We suppose that we are close to the codimension-two TB point $(\mu, \nu) = (0, 0)$ and so explicitly scale μ and ν by ϵ^2 , v by ϵ and time by ϵ^{-1} , where $\epsilon \ll 1$. The resulting scaled equation is

$$\ddot{v} = \mu v + A|v|^2v + \epsilon(\nu \dot{v} + C(v\dot{v} + \bar{v}\dot{v})v + D|v|^2\dot{v}) + \mathcal{O}(\epsilon^2). \quad (3)$$

In this paper only the dynamics that persist in the limit $\epsilon \rightarrow 0$ will be of interest. Equation (3) shows that in this limit, the coefficient B drops out and does not affect the states we study or their stability. In most of the analysis below, we find it convenient to approach this limit by setting $\nu = \pm 1$ and allowing ϵ to be small; effectively, we use (μ, ϵ) as unfolding parameters, and the original parameters in this case are $(\epsilon^2\mu, \pm\epsilon^2)$.

In addition, we find it more convenient to work with the equations in the form of a third-order system of ODEs for the variables (r, s, L) ,

$$\dot{r} = s, \quad \dot{s} = \mu r + Ar^3 + \epsilon(\nu + Mr^2)s + \frac{L^2}{r^3}, \quad \dot{L} = \epsilon L(\nu + Dr^2), \quad (4)$$

where $M = 2C + D$ and we have written $v = re^{i\phi}$ with $L \equiv r^2\dot{\phi}$ [14]. This form of the problem is a consequence of rotational invariance of Eq. (3).

Solution (Abbreviation)	Properties
Steady state (SS)	$(r, s, L) = (*, 0, 0)$
Traveling wave (TW)	$(r, s, L) = (*, 0, *)$
Standing wave (SW)	$(r, s, L) = (**, **, 0)$
Modulated wave (MW)	$(r, s, L) = (**, **, **)$

Table 1. Properties of the four basic solutions of Eq. (4), where * indicates a constant non-zero value, while ** indicates a time-dependent non-zero value.

The four known types of solution (see table 1) are steady-states (SS), for which $s = L = 0$ and $r = \sqrt{-\mu/A}$, traveling waves (TW), for which $s = \dot{L} = 0$, $r = \sqrt{-\nu/D}$ and $L = \pm \frac{\nu}{D} \sqrt{-(\mu - (A/D)\nu)}$, standing waves (SW), which are periodic orbits with $L = 0$, and modulated waves (MW), which are periodic orbits with $L \neq 0$.

In the limit of small ϵ , DK derived averaged equations for $E \equiv \frac{1}{2}s^2 + \frac{1}{2}\frac{L^2}{r^2} - \frac{1}{2}\mu r^2 - \frac{1}{4}Ar^4$ and L ,

$$\dot{E} = \epsilon f(E, L^2) + \mathcal{O}(\epsilon^2) \quad \text{and} \quad \dot{L} = \epsilon Lg(E, L^2) + \mathcal{O}(\epsilon^2), \quad (5)$$

where the functions f and g were expressed as elliptic integrals. The SS, SW, TW and MW solutions were found as roots of $f = Lg = 0$. Truncated at $\mathcal{O}(\epsilon)$, these second-order ODEs cannot have chaotic solutions. The derivation of (5) relied on a separation of time-scales between the period of closed orbits in (4) and the time-scale over which these orbits evolve. This separation does not hold near the homoclinic bifurcations of MW since the period of the MW diverges to infinity; it is near the homoclinic bifurcations of MW that we find chaotic solutions.

We recall briefly some of the relevant results of DK. The trivial solution $v = 0$ is stable when μ and ν are both negative; it loses stability in a pitchfork bifurcation (creating a circle of SS) when $\mu = 0$ and in a Hopf bifurcation (creating SW and TW) when $\nu = 0$ with $\mu < 0$. The Hopf bifurcation from TW to MW (TW-Hopf) occurs when

$$\mu = \frac{3M - 5D}{2M - 4D} \frac{A}{D} \nu, \quad \text{with } \mu < \frac{A}{D} \nu, \quad (6)$$

while the pitchfork bifurcation from SS to TW (SS-pf) occurs when

$$\mu = \frac{A}{D}\nu, \quad \text{with } A\mu < 0. \quad (7)$$

The SW solution is destroyed in a heteroclinic bifurcation (SW-het) when it collides with the SS equilibria at

$$\mu = \frac{5A}{M}\nu + \mathcal{O}(\epsilon), \quad \text{with } A > 0, \mu < 0, \quad (8)$$

while the MW solution is destroyed in a homoclinic bifurcation (MW-hom) when it collides with the TW branch at

$$\mu = \frac{3M - 5D}{2M} \frac{A}{D}\nu + \mathcal{O}(\epsilon), \quad \text{with } A > 0, \mu < 0 \text{ and } 0 < \frac{D}{M} < \frac{1}{5}. \quad (9)$$

Finally, there is the possibility of a pitchfork bifurcation from SW to MW (SW-pf). The expression for the location of this bifurcation involves computing elliptic integrals, but in the special case $\frac{D}{M} = \frac{1}{5}$, it occurs along the half-line

$$\mu = \frac{A}{D}\nu + \mathcal{O}(\epsilon), \quad \text{with } A > 0, \mu < 0 \text{ and } \frac{D}{M} = \frac{1}{5}. \quad (10)$$

Thus in the special case $\frac{D}{M} = \frac{1}{5}$ the last four of these bifurcations (SS-pf, SW-het, MW-hom and SW-pf) occur along lines that are tangent to $\mu = A\nu/D$ as $\epsilon \rightarrow 0$. This four-fold degeneracy is lifted when ϵ is finite, i.e., at any finite distance from the TB point, or by changing the value of D/M . To understand the transition between regions II⁻ and III⁻ in DK [14, figure 5] we need, therefore, to go beyond the analysis of DK and understand how the degeneracy is lifted for small but finite values of ϵ , i.e., we need to determine the role of the higher order terms in eqs. (7)–(10), and to investigate which other bifurcations or solutions might occur.

Before discussing the new results, we consider the issue of the stability of the MW at the homoclinic bifurcation when they collide with TW. DK discussed the two Floquet multipliers of the MW derived from the second-order averaged equations (5), and concluded that in the case $A > 0$, $D < 0$, $M < 0$ and $\frac{1}{5} < \frac{D}{M} < \frac{1}{2}$, stable MW are created in a supercritical Hopf bifurcation from TW, with the branch of stable MW terminating in a pitchfork bifurcation on SW (figure 1a). In the case $0 < \frac{D}{M} < \frac{1}{5}$, there is still a branch of stable

MW created in a supercritical Hopf bifurcation from TW, but the MW are destroyed in a homoclinic bifurcation on the TW branch (figure 1b). Within the second-order averaged equations, the MW are supposed to be stable at the homoclinic bifurcation since the negative eigenvalue of TW is greater in magnitude than the positive. However, in the third-order equations (4), between the Hopf and homoclinic bifurcations, the TW have one negative real eigenvalue and two eigenvalues with positive real part (since they started stable and then underwent a Hopf bifurcation), and at the point of the MW-hom bifurcation, one can show that the two positive eigenvalues are real. Generically, periodic orbits that approach a homoclinic bifurcation involving an equilibrium point with one negative and two distinct positive real eigenvalues are not stable [17], and so the MW cannot be stable at the homoclinic bifurcation. The change from stable MW (at the Hopf bifurcation) to unstable MW (at the homoclinic bifurcation) was therefore not captured by the analysis of DK.

These considerations reveal that there are two issues to be resolved in understanding of the Takens–Bogdanov normal form with $O(2)$ symmetry: how do the four coincident bifurcations split apart when higher-order terms are taken into consideration, and how do the MW become unstable before they collide with the TW branch. To explore these issues, we focus on the interesting case $A = 1$, $D = -1$ and $M \approx -5$. There is a third consideration, which is how the homoclinic bifurcation of MW changes into a heteroclinic bifurcation involving SS and SW further away from the codimension-two point, a situation we consider briefly at the end of section 3.

3 Numerical results near the Takens–Bogdanov point

We have carried out a series of numerical experiments on the ODEs (4) using the AUTO2000 [18] suite of continuation software to follow several of the bifurcations, including the SW-het, MW-hom and SW-pf bifurcations, as well as the first period-doubling of MW (MW-pd) and a saddle-node of MW (MW-sn). For these computations we fixed $\nu = \pm 1$ ($\nu = +1$ is the interesting case) and used μ and ϵ as our unfolding parameters; the results below are presented as functions of $\epsilon\nu$ and $\epsilon(\mu - \frac{A}{D}\nu)$, chosen so that the SS-pf bifurcation line is horizontal.

The results are shown in figures 2 and 3. Schematic version of the unfolding

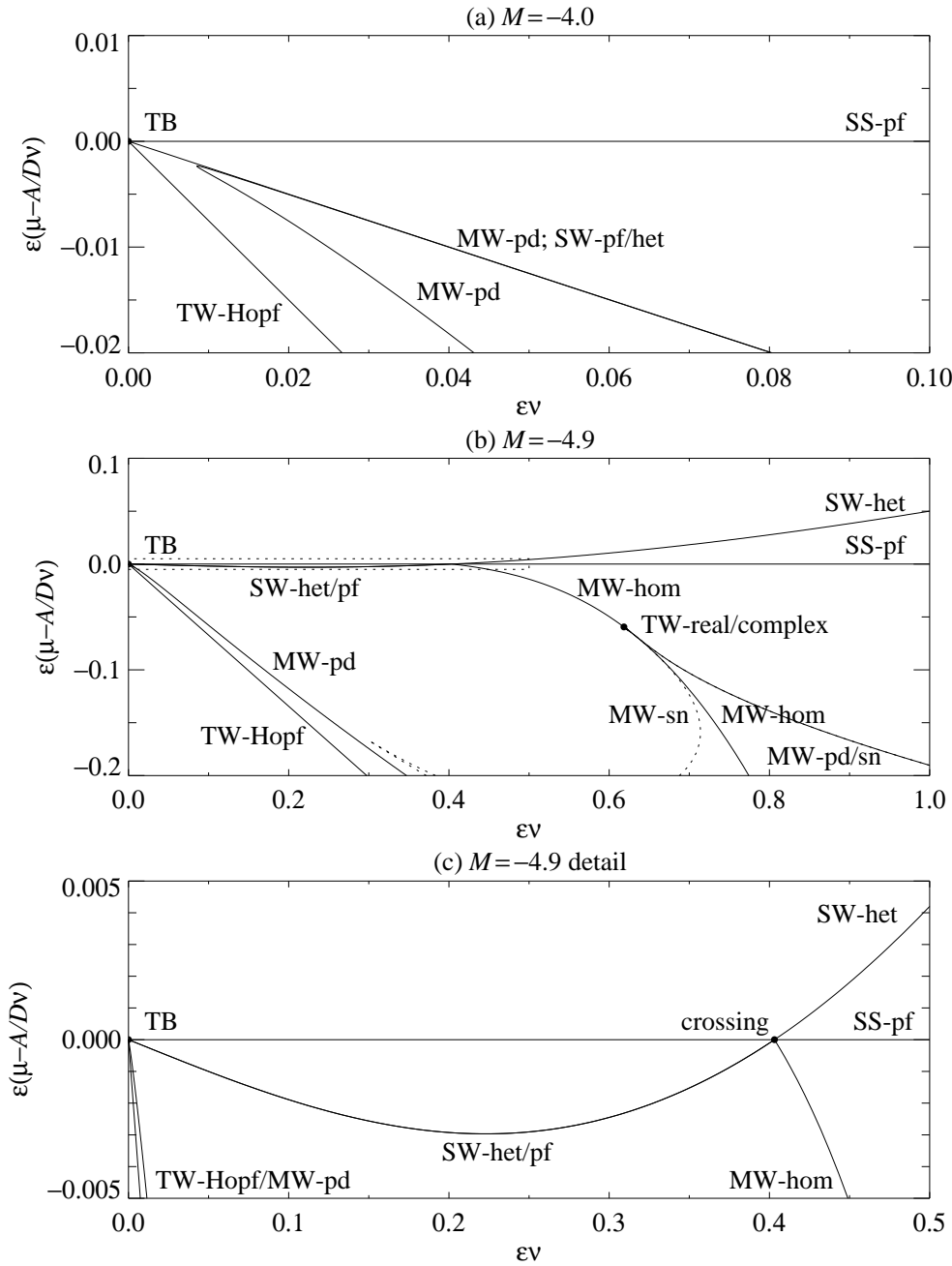


Figure 2. Computed unfolding diagrams for Eqs. (4), with $A = 1$ and $D = -1$, and (a) $M = -4.0$, (b) $M = -4.9$, (c) $M = -4.9$ (detail of the dotted box region in b). We plot $\epsilon\nu$ on the horizontal axis and $\epsilon(\mu - \frac{A}{D}\nu)$ on the vertical axis, so that the line of SS-pf is horizontal. Some of the lines are too close together (for example, SW-pf/SW-het, and MW-pd/MW-sn) to be resolved in this diagram; a schematic drawing of the unfolding diagram is therefore shown in figure 4. The crossing of the SS-pf and SW-het bifurcations is clearly seen in (b), and in more detail in (c). The MW-hom line emerges from the crossing point.

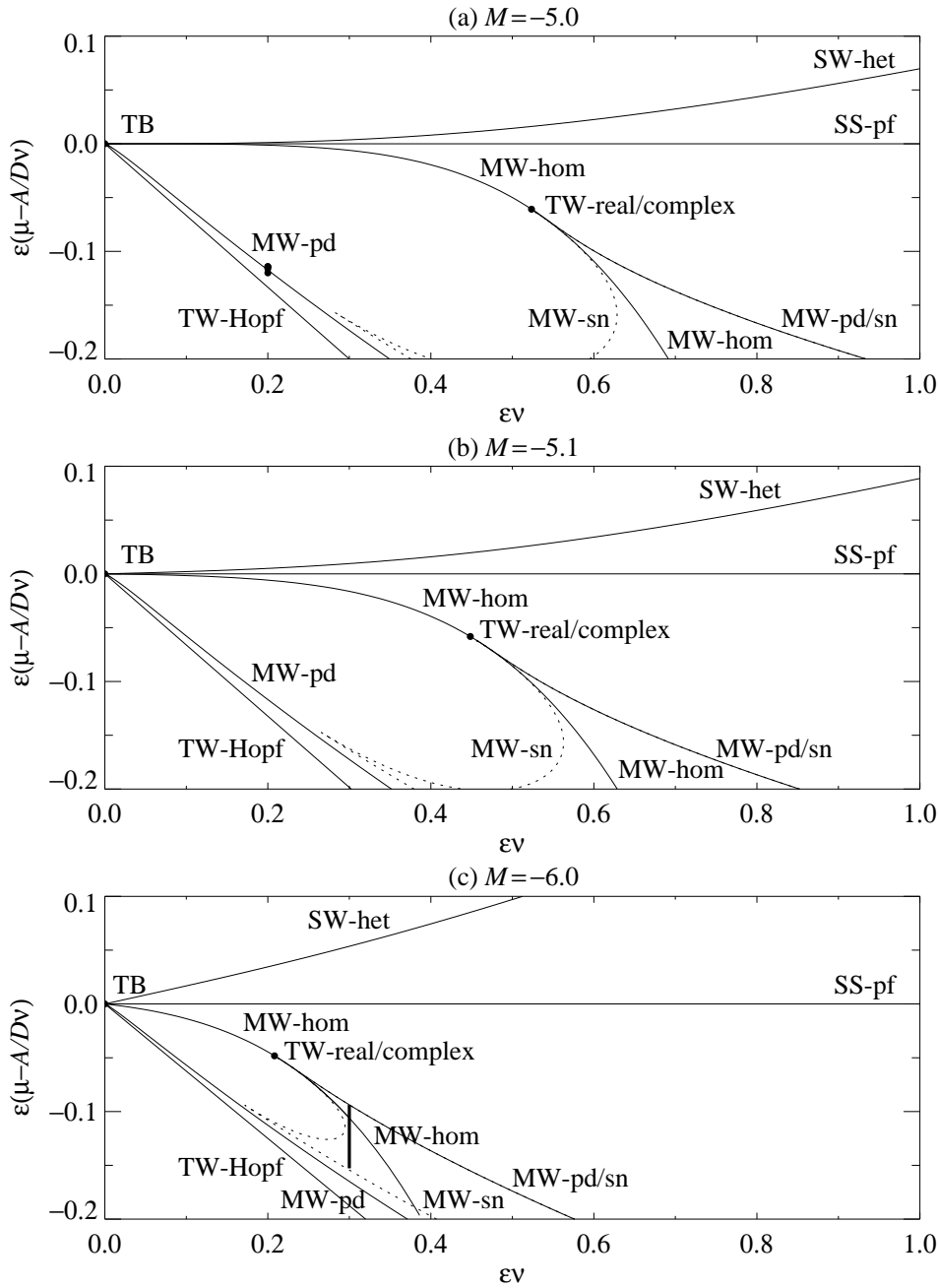


Figure 3. Continuation of figure 2: computed unfolding diagrams for Eqs. (4), with $A = 1$ and $D = -1$, and (a) $M = -5.0$, (b) $M = -5.1$, (c) $M = -6.0$. In (a), with $M = -5.0$, the lines of SS-pf, SW-het and MW-hom are tangent at the TB point, and the line of SW-pf has shrunk to zero. On the MW-hom line, where MW are homoclinic to TW, the leading eigenvalues of TW change from being real to complex, and secondary lines of MW-sn and MW-pd (demarcating the edges of the MW period-doubling cascade) emerge. In (a), the dots at $\epsilon\nu = 0.2$, below the ‘MW-pd’ label, indicate the parameter values in figure 6. In (c), the vertical bar at $\epsilon\nu = 0.3$ indicates the range between the leftmost and rightmost saddle-node bifurcations in figure 8(b).

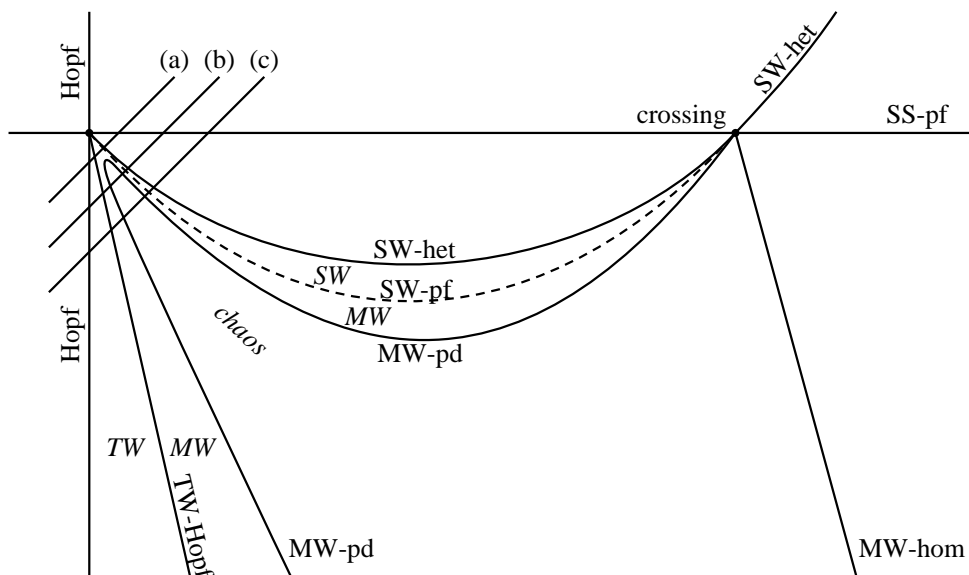


Figure 4. Schematic drawing of the unfolding diagram, for M just above -5 , and including the crossing of the SS-pf and SW-het bifurcations. The loop of MW-pd bifurcations comes close to the TB point, but does not connect to it, instead turning away and apparently ending at the crossing point, where the line of MW-hom bifurcations begin. As M decreases below -5 , the crossing point moves to the left and vanishes when it collides with the TB point, allowing the MW-pd and MW-hom bifurcation lines to connect to the TB point (see figure 3b,c). Regions of stable solutions (TW, MW, chaos and SW) are indicated in italics.

and bifurcation diagrams are shown in figures 4 and 5, and examples of numerical solutions of (4), showing stable MW, period-doubled MW as well as chaotic solutions, are in figures 6 and 7. Finally, figure 8 shows how the MW-hom bifurcation changes to a heteroclinic bifurcation, with snaking behavior, further from the TB point.

These calculations were difficult to perform (especially for small ϵ), and we took great care in choosing the various parameters in AUTO that control the accuracy of the results. One reason for the difficulty is that some of the bifurcations are exceedingly close to each other; furthermore, close to the Takens–Bogdanov point, the -1 Floquet multiplier at the period-doubling bifurcation is nearly degenerate, suggesting that there is a possibility of a torus (Neimark–Sacker) bifurcation from the MW, although we were not able to detect this with confidence. As a consequence of having a second Floquet mul-

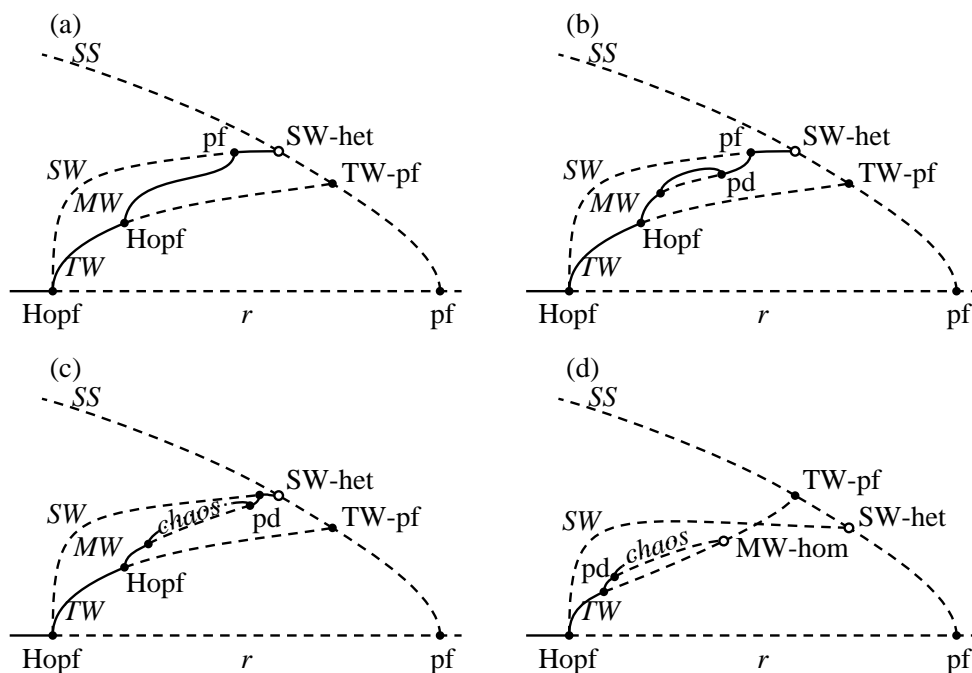


Figure 5. Schematic bifurcation diagrams taken along the cuts indicated in figure 4. (a) and (b): with $M = -4.0$, taken close to the TB point (see figure 1a), and slightly further away, showing how an interval of MW-period doubling comes in. (c): with $M = -4.9$, there is a period-doubling cascade leading to chaotic MW trajectories, but MW must be restabilized before the branch ends in the SW-pf bifurcation; this occurs through a MW-pd bifurcation. (d): with $M = -5.1$, the SW-het and TW-pf bifurcations have changed order on the SS branch. The MW branch ends in the MW-hom bifurcation when unstable MW collide with TW, but the chaotic MW persist (contrast with figure 1b).

tiplier close to the unit circle, the stable MW (and chaotic solutions) are only just stable for small ϵ , and when following solutions using time-stepping, very small changes in parameter value were required if trajectories are not to fall off the stable branch and diverge to infinity.

With $M > -5$ ($M = -4.0$ and -4.9 in figure 2a–c, shown schematically in figures 4 and 5), the MW branch exists between the TW-Hopf and the SW-pf bifurcations. The second of these is almost immediately followed by the SW-het bifurcation, in which the SW branch is destroyed when it collides with the SS equilibria, consistent with the analysis of DK (figure 1a). However, it is clear from figure 2(b,c) that the curves of SW-het and SW-pf begin below the line of SS-pf but bend upwards and there is a codimension-two crossing point at which these bifurcations coincide. We analyse this crossing point in detail in

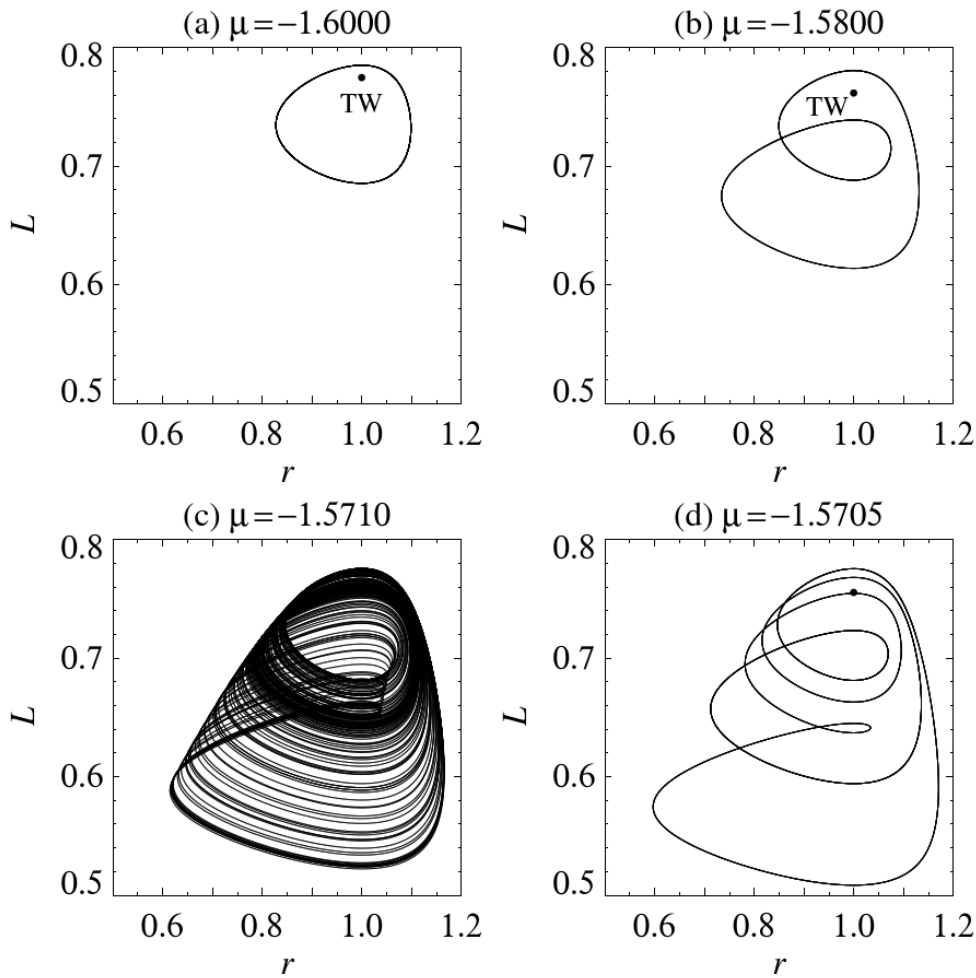


Figure 6. Examples of stable solutions of Eqs. (4) in the (r, L) plane, with $A = 1$, $M = -5$, $D = -1$, $\nu = 1$, $\epsilon = 0.2$ and (a) $\mu = -1.6000$ (stable MW), (b) $\mu = -1.5800$ (period-doubled MW), (c) $\mu = -1.5710$ (chaotic MW), (d) $\mu = -1.5705$ (MW in a period 5 window). This range of parameter values is indicated in figure 3(a). The TW equilibrium point is indicated.

section 4, but a summary is shown in figure 4: the SW-het bifurcation continues through this point, while the SW-pf line terminates there and a line of MW-hom bifurcations begins there. We also found a line of MW-pd bifurcations that begins at the crossing point; we present stable period-doubled and chaotic MW at $M = -5$ in figure 6, and present evidence in section 4 for the origin of this line.

Figure 5 shows schematic bifurcation diagrams taken along the cuts indi-

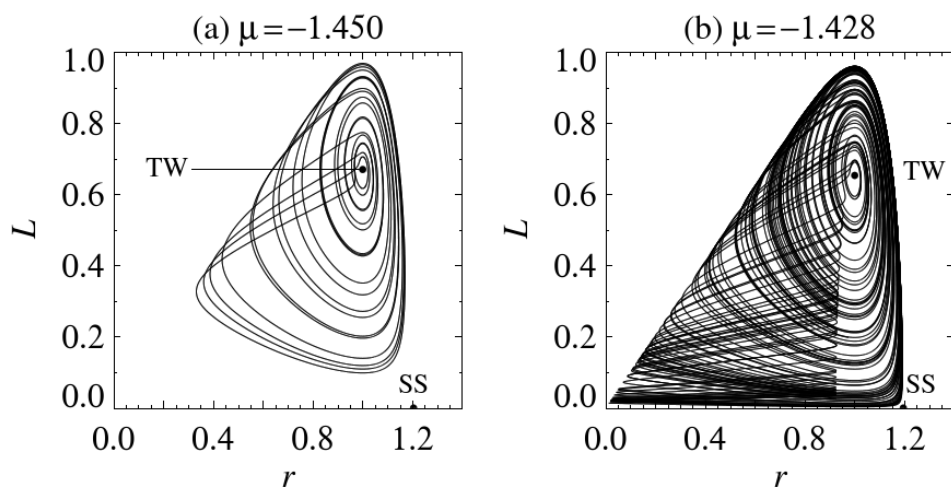


Figure 7. Examples of stable solutions of Eqs. (4) in the (r, L) plane, with $A = 1$, $M = -5$, $D = -1$, $\nu = 1$, $\epsilon = 1$ and (a) $\mu = -1.450$ (chaotic MW near a MW-homoclinic bifurcation with TW), (b) $\mu = -1.428$ (chaotic MW near a MW-heteroclinic bifurcation with TW, SS and SW); these parameter values are outside the range of figure 3(a). The TW and SS equilibrium points are indicated; SW lie in the plane $L = 0$, with $0 \leq r \leq 0.9$.

cated schematically in figure 4. These cuts are notionally taken across the unfolding diagram at a small but non-zero distance from the TB point, and show how the chaotic dynamics inevitably approaches the TB point as M is decreased through $M = -5$.

Figure 5(a) shows the DK scenario. Further from the TB point, a bubble of period-doubled MW develops (figure 5b); further still, there is a period-doubling cascade leading to chaotic MW, followed by an inverse cascade back to MW (figure 5c).

The DK scenario is always correct for $M > -5$, provided that the cut is taken progressively closer to the TB point as M approaches -5 . But, as M passes below -5 (figure 5d), the SW-het emerges from the TB point above instead of below to SS-pf line, implying the crossing point has moved into the TB point, the SW-het and TW-pf bifurcations have changed order, and the SW-pf and final MW-pd bifurcations have vanished and been replaced by the MW-hom bifurcation, i.e., the location of the termination of the MW on the TW branch. However, the initial MW-pd bifurcation survives as does the period-doubling cascade leading to chaotic MW. Figure 5(d) should be contrasted with the DK scenario (figure 1b), where there is no chaos. This is

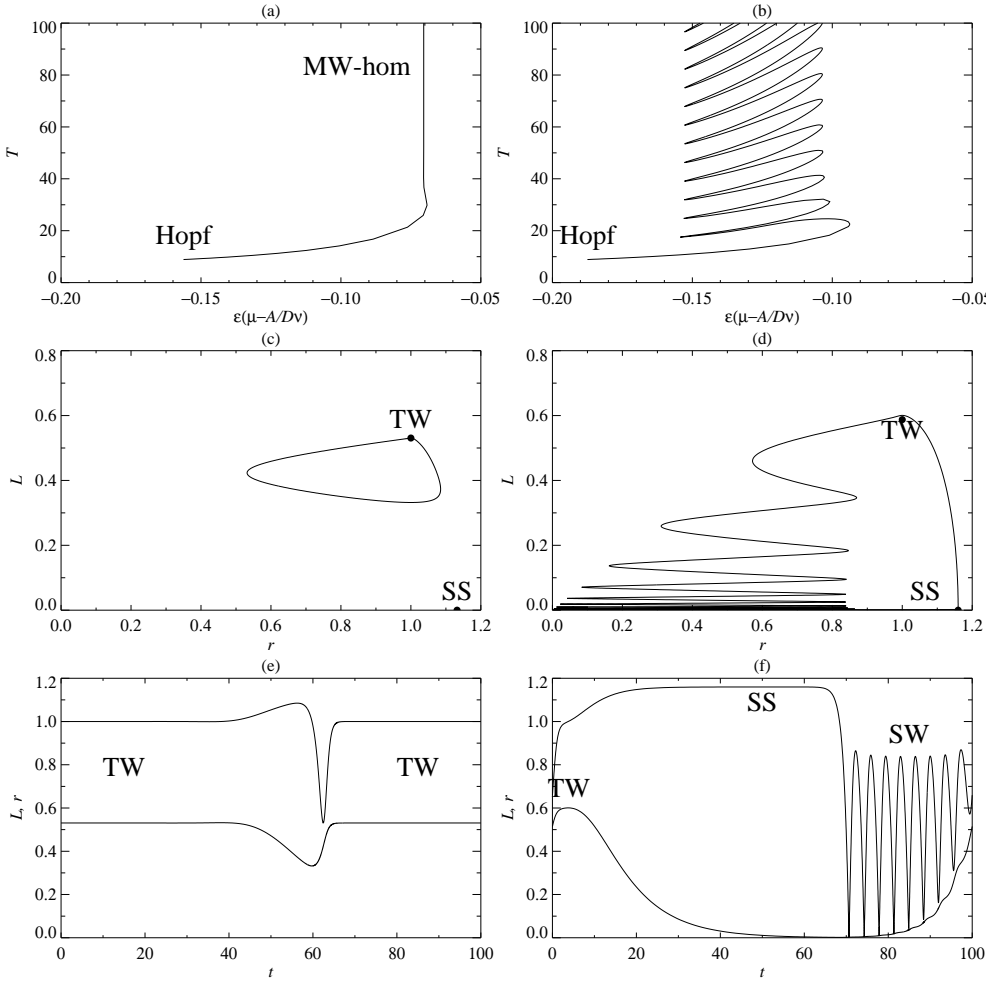


Figure 8. Examples of MW solutions of Eqs. (4) with $M = -6$ and the other parameters as in figure 3(c) found using AUTO. Left column: $\epsilon = 0.25$; right column: $\epsilon = 0.30$. With $\epsilon = 0.25$, the MW are produced at a Hopf bifurcation and terminate in a homoclinic bifurcation involving the TW saddle-focus equilibrium point. Panel (a) shows the period T of the MW as a function of $\epsilon(\mu - \frac{A}{D}\nu)$. The MW solution close to the MW-hom bifurcation is shown in (c) (with period $T = 100$ and $\mu = -1.2816295$), and a time series is shown in (e), with the top line indicating $r(t)$ and the bottom line the corresponding $L(t)$. With $\epsilon = 0.30$, the MW branch still originates in a Hopf bifurcation but subsequently begins to snake back and forth as the MW winds up around the SW periodic orbit (panel (b)). The extent of this snaking, i.e., the distance between the leftmost and rightmost saddle-node bifurcations, is indicated in figure 3(c); there are also period-doubling bifurcations. The MW solution, shown in (d,f) with period $T = 100$ and $\mu = -1.3451861$, approaches the TW and SS equilibria and the SW periodic orbit (cf. [15, 16]).

because the averaged equations used in DK cannot predict the presence of MW period-doubling. The reason for this difficulty is fundamental: the averaging technique replaces a two-torus in (2) by an equilibrium point in (5), and this equilibrium point is identical for all trajectories on this torus, whether periodic or quasiperiodic.

The secondary codimension-two bifurcation point, at which the SW-het and TW-pf bifurcation lines cross, therefore holds the key to resolving the first of the two difficulties with the DK results. The evidence presented so far shows that the crossing point moves to the TB point as M decreases through -5 , and vanishes at $M = -5$. For $M < -5$, all the bifurcation lines that connect to the crossing point will then connect to the TB point instead. In section 4, we show that this includes a MW-pd bifurcation, allowing a consistent interpretation of the numerical results (although we have been unable to continue numerically the line of MW-pd bifurcations all the way to the crossing point.)

We conclude this section by showing some period-doubled and chaotic solutions of Eqs. (4) as well as homoclinic and heteroclinic solutions. In figure 6, we take $M = -5$ and $\epsilon = 0.2$, and show the progression from (a) MW to (b) period-doubled MW to (c) chaotic MW. We also show in figure 6(d) a period 5 MW in a periodic window. The range of parameter values is indicated in figure 3(a). Although these computations are for $M = -5$, we find similar solutions with M just above and just below $M = -5$, thereby providing evidence for the region labeled ‘chaos’ in the schematic diagrams in figure 4 and the initial progress from stable MW to chaos summarized in figure 5(c,d). The termination of the MW branch is too delicate for numerical computation with very small ϵ , although we have been able to find chaotic solutions for ϵ as small as 0.05.

In figure 7, we take $M = -5$ and $\epsilon = 1$, further from the TB point, and show (a) chaotic solutions close to a Shil’nikov homoclinic bifurcation involving the TW saddle-focus, and (b) chaotic solutions close to a heteroclinic connection between TW, SS and SW. For the parameter values in (a), the TW equilibrium point has eigenvalues $0.07627 \pm 0.65395i$ and -4.15255 , with contraction being greater than expansion, consistent with the chaos being stable.

To understand the behavior in figure 7(b) in more detail we show in figure 8(a,c,e) the MW solutions corresponding to $M = -6$ and $\epsilon = 0.25$. The figure shows that in this case the MW branch terminates by forming a homo-

clinic connection with the TW equilibrium point. Figure 8(b,d,f) shows that when $\epsilon = 0.30$ the MW terminate instead in a heteroclinic connection with the SS equilibrium point and the SW periodic orbit. Specifically, figure 8(d,f) demonstrates that the SW in the plane $L = 0$ are unstable with respect to TW perturbations; since the TW are themselves unstable to MW, the trajectory spirals away from $L = 0$ towards MW but the modulation takes the trajectory back towards SS and hence the $L = 0$ invariant plane. In this plane the SS is unstable and solutions are attracted to SW. The process then repeats. Evidently the chaotic solution is associated with the resulting connection from SW to SW such as occurs in the Shil'nikov–Hopf bifurcation [19]. This generic situation is modified here by the fact that the SW lie in the $L = 0$ invariant plane with robust trajectories from SS to SW. The associated bifurcation diagram in figure 8(b) exhibits snaking associated with the addition of more and more turns around the SW limit cycle. The period T of the associated MW diverges within a finite interval of $\epsilon(\mu - A/D\nu)$ instead of a single value as in figure 8(a), a consequence of the structural stability of the intersection between the 2D unstable manifold of SW and the 2D stable manifold of the SW within $L = 0$.

The change from homoclinic to heteroclinic behavior shown in figure 8 occurs beyond the region of validity of the normal form (it does not connect to the TB point), and is present for M above and below $M = -5$. However, the resulting phase portraits greatly resemble those identified in higher-dimensional systems [15, 16] and even in partial differential equations (PDEs) [8], suggesting that similar transitions occur in these systems and that these may in fact be captured by the normal form (4) provided that averaging is eschewed. For this purpose it would be of particular interest to investigate the properties of the full third-order normal form (2). In contrast, the SW chaos observed in the PDEs describing double-diffusive convection is not captured by this normal form since it takes place in the $L = 0$ invariant subspace – the description of this type of chaos requires that the leading eigenvalues of SS at SW-het are complex, something that occurs only a finite distance from the TB codimension-two point [20]. Note that this picture provides a natural construction for a homoclinic connection of a strange invariant set in $L = 0$ to itself [16].

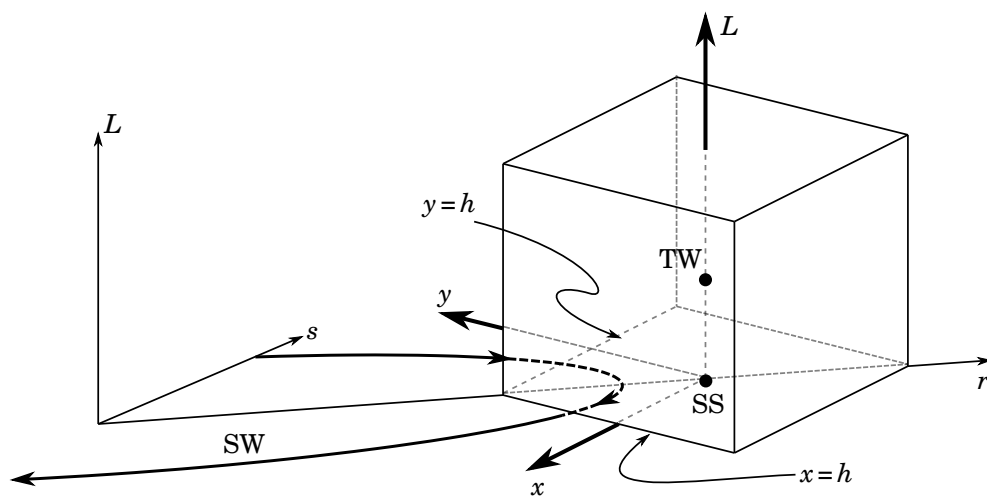


Figure 9. Schematic diagram of the original (r, s, L) coordinate system and the new (x, y, L) coordinate system based at the SS equilibrium point. The x and y axes point, respectively, along the unstable and stable eigendirections of the SS equilibrium within the $L = 0$ plane. The SW periodic orbit lies in the $L = 0$ plane and approaches SS from the positive y direction, and leaves in the positive x direction. The illustration has $\alpha < 0$ so TW exist, and $\kappa < 0$ so SW exist. The flow defines a map from the plane $y = h$ (one of the back faces of the box) to itself.

4 Analysis near the crossing point

We derive a two-dimensional map that describes the dynamics of the third-order ODE (4) near the codimension-two crossing point seen in figure 2(c) and in figure 4. At this point, the heteroclinic bifurcation where the SW periodic orbit collides with the SS equilibria coincides with the pitchfork bifurcation, where TW are created from SS .

For this derivation, we locate the origin of a three-dimensional coordinate system (x, y, L) at the SS equilibrium at $(r, s, L) = (\sqrt{-\mu/\bar{A}}, 0, 0)$, with x along the unstable manifold within the $L = 0$ plane, y along the stable manifold within the same plane, and L as before (see figure 9). We orient the coordinate system so that, close to the global bifurcation, the SW periodic orbit approaches SS from the positive y direction, and leaves in the positive x direction.

The derivation proceeds along standard lines, but with the complication that we allow a pitchfork bifurcation from the SS equilibrium, cf. [19, 21, 22]. We define a small neighborhood of the SS by $|x| \leq h$ and $|y| \leq h$, where h is small, and consider the dynamics within this neighborhood, linearizing in the

(x, y) plane, but keeping nonlinear terms in the L direction:

$$\dot{x} = \lambda_+ x, \quad \dot{y} = \lambda_- y, \quad \dot{L} = \alpha L + L^3, \quad (11)$$

where λ_+ and λ_- are the positive and negative eigenvalues of SS with eigen-directions within the $L = 0$ plane, α is the eigenvalue corresponding to the L direction (so $\alpha = 0$ at the pitchfork bifurcation, when $\mu = A\nu/D$ from (7)), and we have rescaled L to set the coefficient of the cubic term to +1 (so that TW exist when $\alpha < 0$). The TW then satisfy $x = y = 0$ and $L^2 = -\alpha$, and the stable manifold of TW intersects the plane $y = h$ at $x = 0$, $L^2 = -\alpha$.

Trajectories enter the neighborhood with $y = h$, and initial values $x = x_0$ and $L = L_0$. We solve (11) to find

$$x(t) = x_0 e^{\lambda_+ t}, \quad y(t) = h e^{\lambda_- t}, \quad L(t) = L_0 \sqrt{\frac{\alpha e^{2\alpha t}}{\alpha + L_0^2 (1 - e^{2\alpha t})}}. \quad (12)$$

Trajectories leave the neighborhood when $x = h$ at time $T = \frac{1}{\lambda_+} \log\left(\frac{h}{x_0}\right)$. At this time, the y and L coordinates are:

$$y(T) = h \left(\frac{x_0}{h}\right)^{\delta_{SS}}, \quad L(T) = L_0 \sqrt{\frac{\alpha (x_0/h)^{2\delta_L}}{\alpha + L_0^2 (1 - (x_0/h)^{2\delta_L})}}, \quad (13)$$

where $\delta_{SS} = -\lambda_-/\lambda_+$ and $\delta_L = -\alpha/\lambda_+$. For this problem, it can be shown that δ_{SS} tends to 1 from above in the limit $\epsilon \rightarrow 0$. We focus on the case where the crossing point moves close to the Takens–Bogdanov point as $M \rightarrow -5$ from above, and we choose the time-scale so that $\lambda_+ = 1$, i.e., $\delta_L = -\alpha$ and suppose that $\alpha < 0$ ($\delta_L > 0$).

The positive branch of the unstable manifold of SS then leaves the neighborhood at $x = h$, $y = 0$ and $L = 0$, and returns at $x = -\kappa$, $y = h$ and $L = 0$, where κ is a parameter that controls how close we are to the global bifurcation: we choose the parameter so that SW exist when $\kappa < 0$, before the global bifurcation, and that SW are destroyed in the global bifurcation at $\kappa = 0$. The negative branch of the unstable manifold of SS leaves the neighborhood with $x < 0$ and escapes from the domain of the map.

To see the connection between the ODE and the map parameters, in figure 4, the line $\alpha = 0$ is labeled SS-pf, and the line $\kappa = 0$ is labeled SW-het. The

$\kappa < 0$, $\alpha < 0$ quadrant contains the lines SW-pf, MW-pd and MW-hom. At the crossing point, where $(\kappa, \alpha) = (0, 0)$, we have $\delta_{SS} > 1$. As $M \rightarrow -5$ and the crossing point moves closer to the TB point, $\delta_{SS} \rightarrow 1^+$.

Trajectories that leave the neighborhood of SS at $(h, y(T), L(T))$, close to the positive branch of the unstable manifold, return to the neighborhood at (x', h, L') , where, to leading order in a Taylor series expansion, we have

$$x' = -\kappa + Ey(T) + FL^2(T), \quad L' = GL(T). \quad (14)$$

The constants E , F and G are properties of the global flow, and must satisfy $E > 0$ (since trajectories in the plane $L = 0$ cannot cross) and $G > 0$ (since trajectories cannot cross the $L = 0$ subspace). The form of this map respects the $L \rightarrow -L$ symmetry of (4).

Putting this together results in a map $(x, h, L) \rightarrow (x', h, L')$, where

$$x' = -\kappa + Ex^{\delta_{SS}} + \frac{FL^2x^{2\delta_L}}{1 + \frac{L^2}{\alpha}(1 - x^{2\delta_L})}, \quad L' = \frac{GLx^{\delta_L}}{\sqrt{1 + \frac{L^2}{\alpha}(1 - x^{2\delta_L})}}, \quad (15)$$

and we have dropped the 0 subscripts and absorbed h into the definitions of the other constants and into the scaling of the x coordinate. By further scaling L and α , it is possible to set $F = \pm 1$.

Fixed points of the map (15) correspond to periodic orbits (SW and MW) in the differential equations. Within the $L = 0$ subspace, we have SW at $(x_{SW}, 0)$, which satisfy:

$$\kappa = -x_{SW} + Ex_{SW}^{\delta_{SS}}, \quad (16)$$

confirming that SW exist for $\kappa < 0$ when $\delta_{SS} > 1$. The stability of SW are given by the two Floquet multipliers (eigenvalues of the Jacobian matrix), which are $\tilde{E} = \delta_{SS}Ex_{SW}^{\delta_{SS}-1}$ and $Gx_{SW}^{\delta_L}$. Since we expect SW to be stable within the $L = 0$ subspace, we deduce that \tilde{E} must satisfy $0 < \tilde{E} < 1$, and since this is true even in the limit $\epsilon \rightarrow 0$ ($\delta_{SS} \rightarrow 1$), we must also have $0 < E < 1$. Writing \tilde{E} in this way emphasises the fact that \tilde{E} is only a weak function of x when δ_{SS} is close to 1, and in the limit $\epsilon \rightarrow 0$ ($\delta_{SS} \rightarrow 1^+$), $\tilde{E} = E$.

The second multiplier gives the location of SW-pf, where SW lose stability to MW in a pitchfork bifurcation. Solving the equation $Gx_{SW}^{\delta_L} = 1$ results in

a relation between κ and α for the location of SW-pf:

$$\kappa_{\text{SW-pf}} = EG^{\delta_{SS}/\alpha} - G^{1/\alpha}. \quad (17)$$

Since SW exist for $\kappa < 0$, and evidence in figure 2(c) and figure 4 suggests that the line of SW-pf connects to the codimension-two point $(\kappa, \alpha) = (0, 0)$ from the quadrant $\kappa < 0$ and $\alpha < 0$, we require $G > 1$ for the limit of $\kappa_{\text{SW-pf}}$ to be zero when $\alpha \rightarrow 0$ from below. When $\delta_{SS} = 1$, we also require $E < 1$ (as found already above).

The MW periodic orbit can be found as a fixed point of the map (15) with $L \neq 0$. The equation $L' = L$ implies that $G^2 x^{2\delta_L} = 1 + \frac{L^2}{\alpha} (1 - x^{2\delta_L})$. This can be solved in two equivalent ways:

$$\begin{aligned} L^2 &= \delta_L(1 - G^2 x^{2\delta_L}) / (1 - x^{2\delta_L}), \\ x^{2\delta_L} &= (\delta_L - L^2) / (G^2 \delta_L - L^2) \end{aligned} \quad (18)$$

(recall $\alpha = -\delta_L$). Then the equation $x' = x$ reduces to $x = -\kappa + Ex^{\delta_{SS}} + FL^2/G^2$, or $\kappa = -x + Ex^{\delta_{SS}} + F(\delta_L/G^2)(1 - G^2 x^{2\delta_L}) / (1 - x^{2\delta_L})$. Thus, for a given value of x and the parameter $\alpha = -\delta_L$, one can calculate the corresponding value of the parameter κ and of L^2 , for MW with this value of x .

The range of values of x for which MW exist is bounded by $x = G^{-1/\delta_L}$ ($L = 0$), where the MW are created in SW-pf, and $x = 0$ ($L^2 = \delta_L$), where they are destroyed in a homoclinic bifurcation (MW-hom) when they collide with the stable manifold of TW. Since $G > 1$ the upper bound of this range decreases to zero as $\delta_L \rightarrow 0^+$. At the MW-hom bifurcation, we have

$$\kappa_{\text{MW-hom}} = -\alpha F / G^2. \quad (19)$$

Numerical evidence in figure 2(c) and figure 4 suggests that this line is also in the $\kappa < 0$ and $\alpha < 0$ quadrant, and we conclude that $F = -1$.

With this value of F the Jacobian matrix evaluated on the MW branch is:

$$J = \begin{bmatrix} \tilde{E} - \frac{2L^2\delta_L}{G^2x} + \frac{2L^4}{G^4x} & \frac{-2L}{G^4x^{2\delta_L}} \\ \frac{L\delta_L}{x} - \frac{L^3}{G^2x} & \frac{1}{G^2x^{2\delta_L}} \end{bmatrix}, \quad \text{with} \quad \det(J) = \frac{\tilde{E}}{G^2x^{2\delta_L}}, \quad (20)$$

where x and L are the values for the MW, and we have made use of (18) to make these expressions as simple as possible. In these expressions, $\tilde{E} =$

$\delta_{SS}Ex^{\delta_{SS}-1}$. Since $\delta_{SS} > 1$ and $\delta_L = 0$ at the crossing point, it follows that $\det(J) \rightarrow 0$ at this point.

We consider first the possibility of a torus bifurcation from MW; the relevant conditions are $\det(J) = 1$ and $-2 < \text{Trace}(J) < 2$. The first equation implies $x^{\delta_L} = \sqrt{\tilde{E}}/G$. With this value of x , we have $L^2 = \delta_L G^2(1 - \tilde{E})/(G^2 - \tilde{E})$, so

$$\text{Trace}(J) = \tilde{E} + \frac{1}{\tilde{E}} - \frac{2(G^2 - 1)(1 - \tilde{E})\delta_L^2}{(G^2 - \tilde{E})^2 \left(\frac{\sqrt{\tilde{E}}}{G}\right)^{1/\delta_L}}. \quad (21)$$

For small positive δ_L (close to the codimension-two crossing point), we have $\delta_L^2/(\sqrt{\tilde{E}}/G)^{1/\delta_L} \rightarrow \infty$, so the condition $-2 < \text{Trace}(J) < 2$ is not satisfied, and there is no torus bifurcation from MW connecting to the codimension-two point.

We turn now to the period-doubling case. A numerical exploration of the relevant condition, $\det(J) + \text{Trace}(J) + 1 = 0$, suggests that with small δ_L , there are solutions close to the SW-pf bifurcation, with Gx^{δ_L} close to 1 and L close to 0 (in particular, $L^2 \ll \delta_L$). With this in mind, we write the condition $\det(J) + \text{Trace}(J) + 1 = 0$ as

$$\frac{(L^2 + G^2 L^2 - 2\delta_L G^2)(1 + \tilde{E})}{L^2 - \delta_L} = \frac{2(\delta_L G^2 - L^2)L^2}{G^2 x}. \quad (22)$$

With $x \approx (1/G)^{1/\delta_L}$ and $L^2 \ll \delta_L$, this is solved by

$$L^2 \approx \frac{1}{\delta_L} \left(\frac{1}{G}\right)^{\frac{1}{\delta_L}} G^2(1 + \tilde{E}), \quad (23)$$

from which κ can be deduced:

$$\kappa_{\text{MW-pd}} = - \left(1 + \frac{1}{\delta_L}\right) G^{\frac{1}{\alpha}} + E G^{\frac{\delta_{SS}}{\alpha}} \left(1 - \frac{\delta_{SS}}{\delta_L}\right) \quad (24)$$

To obtain this expression we have replaced δ_L by $-\alpha$. This approximate solution satisfies the scaling assumptions that were made in its derivation. There is therefore a line of MW-pd bifurcations connecting to the codimension-two crossing point. Comparing with (17), we see that the bifurcation lines SW-het (creating SW at $\kappa = 0$), SW-pf (creating the MW) and MW-pd (where

the MW lose stability) are all tangent as they approach the codimension-two crossing point. These results have been used to inform the sketch in figure 4.

As $M \rightarrow -5$ (and $\delta_{GS} \rightarrow 1^+$), the crossing point approaches the TB point and brings with it the MW-pd bifurcation found above. Consequently, when $M = -5$, we expect to see the MW-pd bifurcation line emerging from the TB point; this is supported by the numerical evidence in figure 3(a). The map does not apply for $M < -5$ (since there is no crossing point), but numerical evidence (figure 3b,c) indicates that the MW-pd line remains connected to the TB point.

5 Discussion

The presence of chaos near the Takens–Bogdanov point has been of interest ever since the discovery of chaotic dynamics of SW solutions in doubly diffusive convection [20, 23] and its study established its relation to the Shil’nikov scenario, i.e., to the presence of a Shil’nikov orbit between a pair of symmetry-related saddle-points corresponding to unstable steady convection, all within the $L = 0$ invariant subspace of the governing PDEs [6, 20, 24–26]. However, it was discovered in [27] that the SW states are in fact unstable to TW perturbations whenever such waves are permitted by the imposed boundary conditions, a discovery that led to intensive study of the competition between SW and TW in the nonlinear regime in systems with periodic boundary conditions [28–30]. The study of the Takens–Bogdanov bifurcation with $O(2)$ symmetry was the natural next step, undertaken in DK, since this bifurcation brings steady states into the picture as well. The results of the DK analysis were subsequently applied to a number of systems including convection in a magnetic field [5, 31] and rotating convection [32].

However, as shown here, the analysis of DK is incomplete in one important sense, associated with the failure of averaging near global bifurcations.¹ This difficulty has in fact been known for a long time [34]. In particular, it was known that the integrability of many normal forms gives incomplete results in regions near global bifurcations since either higher order terms or those that break normal form symmetry can lead to transverse intersection of stable and

¹DK also omit one of the bifurcation diagrams that arises in region IX[−] of their classification [33].

unstable manifolds and these in turn generate thin regions of chaos near these manifolds. This is the case in the Takens–Bogdanov bifurcation with $O(2)$ symmetry as well, and in particular in the vicinity of the global bifurcation at which the MW branch terminates. The reason is simple: averaging requires that the oscillation period (here the modulation period) remains finite for small ϵ , a condition that breaks down near global bifurcations. In these regions a higher-dimensional analysis is required, and as shown here, period-doubling and chaos may be uncovered. When the homoclinic or heteroclinic tangles are generated by terms breaking normal form symmetry these parameter regions are exponentially thin; this is expected to be the case in the present study as well, and accounts for the difficulty in carrying out numerical work for small ϵ .

Of particular interest in the present case is the fact that some of the resulting complex behavior is present arbitrarily close to the codimension-two Takens–Bogdanov point, i.e., arbitrarily close to the bifurcation. We consider this bifurcation, therefore, to be another example of instant chaos, much as the well-known cases studied by Arneodo *et al.* [35] and Guckenheimer and Worfolk [36]. In contrast the SW chaos referred to above cannot take place arbitrarily close to the TB point. In the 2:1 spatial resonance with $O(2)$ symmetry the heteroclinic cycles present near the codimension-two point are structurally stable [37] and any chaos in this regime is the result of the presence of noise. However, further out from the codimension-two point one finds the same transition scenario as found here, viz. $SS \rightarrow TW \rightarrow MW$ followed by a global bifurcation involving SW [38].

The fact that the full, unaveraged yet truncated normal form does in fact capture some aspects of the chaotic dynamics associated with the termination of MW implies that the normal form contains information beyond that in the averaged equations studied by DK. Evidently it is not necessary to go to higher order in the normal form in order to capture the behavior observed in [8, 15, 16], only to extend the normal form analysis beyond averaging. In contrast, in other normal forms exhibiting global bifurcations [19, 22, 39, 40] the normal forms are intrinsically two-dimensional, at least after symmetry reduction. In these cases complex dynamics appear only when the normal form symmetry is explicitly broken. However, as cautioned by Wittenberg and Holmes [41], the resulting interval of chaos may be much thinner than in the original system from which the normal form was derived.

The fact that averaging fails near global bifurcations such as those discussed here involving the termination of the MW branch is of course well known. This failure originates in the divergence of the oscillation period at the global bifurcation or, as in the present case, the divergence of the modulation period. A common procedure for overcoming this problem is to construct an appropriate return map valid in the neighborhood of this bifurcation and matching the results to those obtained from averaging as one moves away from the global bifurcation. This is the procedure adopted here. In [19] the authors consider a fixed point undergoing a Hopf and a pitchfork bifurcation in close succession in a regime where the mixed mode undergoes a secondary Hopf bifurcation, thereby creating an invariant 2-torus. The authors show that terms that break normal form symmetry generate a sequence of resonances between the primary and secondary Hopf frequencies and mergers of the resonance tongues [42] may result in complex dynamics of Shil'nikov type associated with homoclinic bifurcations that are intertwined with heteroclinic bifurcation. This complex structure results from the break up of the heteroclinic orbit responsible for the destruction of the 2-torus in the normal form. In the problem studied here we find related behavior, including Shil'nikov dynamics. The reason is fundamentally the same: the original system (4) is three-dimensional, but the process of averaging leads to a second order system and hence captures only two of the three eigenvalues required to specify the stability properties of the MW 2-torus completely. These two eigenvalues describe these properties correctly when the averaging procedure is valid because the third eigenvalue vanishes. But in the vicinity of the global bifurcation the third eigenvalue no longer decouples and its sign determines the stability of the MW near its termination. Indeed, we can view the results of this paper as showing that this eigenvalue is in fact negative (so that the MW branch is unstable near its end), despite the fact that the averaged system studied in [14] suggests that it should be stable, based on the two eigenvalues that can be computed using this approach. It is this realization that reconciles the results of the present work and that of DK. In other systems this increase in the dimension of the system near global bifurcations leads to thin regions of chaos, as described, for example, by Guckenheimer [34, 43] and Langford [44].

Acknowledgments

This work was begun in 1993. We thank Marty Golubitsky for encouraging us to publish the results in a timely fashion.

References

- [1] S. Chandrasekhar, *Hydrodynamic and Hydromagnetic Stability*, Clarendon Press, Oxford, 1961.
- [2] E. Knobloch, M. R. E. Proctor, Nonlinear periodic convection in double-diffusive systems, *J. Fluid Mech.* 108 (1981) 291–316.
- [3] L. N. Da Costa, E. Knobloch, N. O. Weiss, Oscillations in double-diffusive convection, *J. Fluid Mech.* 109 (1981) 25–43.
- [4] J. Guckenheimer, E. Knobloch, Nonlinear convection in a rotating layer: amplitude expansions and normal forms, *Geophys. Astrophys. Fluid Dyn.* 23 (1983) 247–272.
- [5] E. Knobloch, On convection in a horizontal magnetic field with periodic boundary conditions, *Geophys. Astrophys. Fluid Dyn.* 36 (1986) 161–177.
- [6] A. M. Rucklidge, Chaos in models of double convection, *J. Fluid Mech.* 237 (1992) 209–229.
- [7] A. M. Rucklidge, N. O. Weiss, D. P. Brownjohn, M. R. E. Proctor, Oscillations and secondary bifurcations in nonlinear magnetoconvection, *Geophys. Astrophys. Fluid Dyn.* 68 (1993) 133–150.
- [8] S. M. Cox, S. Leibovich, I. M. Moroz, A. Tandon, Nonlinear dynamics in Langmuir circulations with $O(2)$ symmetry, *J. Fluid Mech.* 241 (1992) 669–704.
- [9] J. D. Crawford, Amplitude expansions for instabilities in populations of globally coupled oscillators, *J. Stat. Phys.* 74 (1994) 1047–1084.
- [10] M. Golubitsky, V. G. LeBlanc, I. Melbourne, Meandering of the spiral tip: An alternative approach, *J. Nonlin. Sci.* 7 (1997) 557–586.
- [11] J. Guckenheimer, P. Holmes, *Nonlinear Oscillations, Dynamical Systems and Bifurcations of Vector Fields*, Springer, New York, 1983.
- [12] K. Matthies, A subshift of finite type in the Takens-Bogdanov bifurcation with D_3 symmetry, *Documenta Mathematica* 4 (1999) 463–485.
- [13] A. M. Rucklidge, Global bifurcations in the Takens–Bogdanov normal form with D_4 symmetry near the $O(2)$ limit, *Phys. Lett. A* 284 (2001) 99–111.
- [14] G. Dangelmayr, E. Knobloch, The Takens–Bogdanov bifurcation with $O(2)$ symmetry, *Phil. Trans. R. Soc. Lond. A* 322 (1987) 243–279.
- [15] E. Knobloch, D. R. Moore, Minimal model of binary fluid convection, *Phys. Rev. A* 42 (1990) 4693–4709.
- [16] E. Knobloch, D. Moore, Chaotic traveling wave convection, *European Journal of Mechanics B-Fluids* 10 (1991) 37–42.
- [17] Y. Kuznetsov, *Elements of Applied Bifurcation Theory*, Second Edition, Vol. 112 of Applied Mathematical Sciences, Springer-Verlag, New York, 1998.
- [18] E. J. Doedel, R. C. Paffenroth, A. R. Champneys, T. F. Fairgrieve, Y. A. Kuznetsov, B. Sandstede, X. Wang, *AUTO 2000: Continuation and bifurcation software for ordinary differential equations* (with HomCont), Tech. rep., Caltech (2001).
- [19] P. Hirschberg, E. Knobloch, Silnikov–Hopf bifurcation, *Physica D* 62 (1993) 202–216.
- [20] E. Knobloch, D. R. Moore, J. Toomre, N. O. Weiss, Transitions to chaos in two-dimensional double-diffusive convection, *J. Fluid Mech.* 166 (1986) 409–448.
- [21] P. Hirschberg, V. Kirk, E. Knobloch, Equivariant bifurcation analysis of localized patterns in excitable media, *Phys. Lett. A* 172 (1992) 141–147.

- [22] J. H. Siggers, Dynamics of target patterns in low-Prandtl-number convection, *J. Fluid Mech.* 475 (2003) 357–375.
- [23] D. R. Moore, T. J., E. Knobloch, N. O. Weiss, Period doubling and chaos in partial-differential equations for thermosolutal convection, *Nature* 303 (1983) 663–667.
- [24] M. R. E. Proctor, N. O. Weiss, Normal forms and chaos in thermosolutal convection, *Nonlinearity* 3 (1990) 619–637.
- [25] A. M. Rucklidge, Chaos in a low-order model of magnetoconvection, *Physica D* 62 (1993) 323–337.
- [26] A. M. Rucklidge, Chaos in magnetoconvection, *Nonlinearity* 7 (1994) 1565–1591.
- [27] E. Knobloch, A. E. Deane, T. J., M. D. R., Doubly diffusive waves, in: M. Golubitsky, J. Guckenheimer (Eds.), *Multiparameter Bifurcation Theory*, Vol. 56 of *Contemporary Math.*, Amer. Math. Soc., Providence, RI, 1986, pp. 203–216.
- [28] E. Knobloch, Oscillatory convection in binary mixtures, *Phys. Rev. A* 34 (1986) 1538–1549.
- [29] T. Clune, E. Knobloch, Mean flow suppression by endwalls in oscillatory binary fluid convection, *Physica D* 61 (1992) 106–112.
- [30] P. C. Matthews, A. M. Rucklidge, Traveling and standing waves in magnetoconvection, *Proc. R. Soc. Lond. A* 441 (1993) 649–658.
- [31] G. Dangelmayr, E. Knobloch, Interaction between standing and traveling waves and steady-states in magnetoconvection, *Phys. Lett. A* 117 (1986) 394–398.
- [32] E. Knobloch, M. Silber, Traveling-wave convection in a rotating layer, *Geophys. Astrophys. Fluid Dyn.* 51 (1990) 195–209.
- [33] P. Peplowski, H. Haken, Bifurcation with two parameters in two-dimensional complex space. Applications to laser systems, *Physica D* 30 (1988) 135–150.
- [34] J. Guckenheimer, Multiple bifurcation problems of codimension-2, *SIAM Journal on Mathematical Analysis* 15 (1984) 1–49.
- [35] A. Arneodo, P. Coullet, E. Spiegel, C. Tresser, Asymptotic chaos, *Physica D* 14 (1985) 327–347. URL
- [36] J. Guckenheimer, P. Worfolk, Instant chaos, *Nonlinearity* 5 (1992) 1211–1222.
- [37] D. Armbruster, J. Guckenheimer, P. Holmes, Heteroclinic cycles and modulated traveling waves in systems with $O(2)$ symmetry, *Physica D* 29 (1988) 257–282.
- [38] J. Porter, E. Knobloch, New type of complex dynamics in the 1 : 2 spatial resonance, *Physica D* 159 (2001) 125–154.
- [39] V. Kirk, E. Knobloch, A remark on heteroclinic bifurcations near steady state/pitchfork bifurcations, *Int. J. Bifurcation Chaos* 14 (2004) 3855–3869.
- [40] D. Simpson, V. Kirk, J. Sneyd, Complex oscillations and waves of calcium in pancreatic acinar cells, *Physica D* 200 (2005) 303–324.
- [41] R. W. Wittenberg, P. Holmes, The limited effectiveness of normal forms: A critical review and extension of local bifurcation studies of the Brusselator PDE, *Physica D* 100 (1997) 1–40.
- [42] V. Kirk, Merging of resonance tongues, *Physica D* 66 (1993) 267–281.
- [43] J. Guckenheimer, On a codimension-two bifurcation, in: D. A. Rand, L. S. Young (Eds.), *Dynamical Systems and Turbulence*, Vol. 898 of *Lecture Notes in Mathematics*, Springer-Verlag, New York, 1981, pp. 99–142.
- [44] W. F. Langford, A review of interactions of Hopf and steady-state bifurcations, in: G. I. Barenblatt, G. Iooss, D. D. Joseph (Eds.), *Nonlinear Dynamics and Turbulence*, Pitman, London, 1983, pp. 215–237.